#### Research Article

Peng Zhang, Jia Su, Zhen Gao\*, Tianhang Zhang, and Peng Zhang

# Effect of sand-precursor ratio on mechanical properties and durability of geopolymer mortar with manufactured sand

https://doi.org/10.1515/rams-2023-0170 received May 31, 2023; accepted December 27, 2023

Abstract: The geopolymer mortar (GPM) prepared from industrial by-products and alkali activation solution (AAS) is one of the hot spots of current building materials. As a feasible alternative to natural river sand, manufactured sand (MS) alleviates the global ecological pressure. In this study, MS was used for fine aggregate. Sodium hydroxide (NaOH) and sodium silicate (Na<sub>2</sub>SiO<sub>3</sub>) solution were used as AAS. Metakaolin (MK) and fly ash (FA) were used as the precursor to prepare MK-FA-based GPM with MS (MS-GPM), which was of great significance for saving non-renewable resources, mitigating the greenhouse effect, and recycling waste. Numerous studies were conducted to explore the effect of sand–precursor ratio ( $r_{\rm sp}$ ) on mechanical and durability characteristics of MS-GPM. Relationships between compressive strength and tensile or flexural strength were established by linear fitting equation. Finally, analysis of variance (ANOVA) was used to systematically calculate the effect of  $r_{\rm sp}$  on performance. The results indicated that the mechanical strength and impermeability of MS-GPM decreased and crack resistance increased with  $r_{\rm sp}$  from 1 to 5. The strength of MS-GPM was the best when  $r_{\rm sp}$  was 1. With the increase of  $r_{\rm sp}$ , the proportion of MS in MS-GPM increases, and the relative cementitious material decreases, which has an adverse impact on mechanical properties and impermeability. Linear fitting revealed that the compressive strength of MS-GPM was closely related to tensile strength and flexural strength. ANOVA results indicated that  $r_{\rm sp}$  in the range of 1-5 had great effects on the performance of MS-GPM. The aim of this article is to further promote the

**Keywords:** geopolymer mortar, manufactured sand, mechanical performance, durability, analysis of variance

# 1 Introduction

With the acceleration of urbanization, commercialization and industrialization, concrete production has increased exponentially [1]. According to the United Nations, more than 65% of people all the world are expected to live in cities by 2050. As a traditional cementing material, the consumption of cement is very large. In 2021, global cement production reached 4 billion tons. Taking the ordinary Portland cement (OPC) production process as an example, the raw material mainly limestone in the process of calcination and the burning of fossil fuels will generate large amounts of carbon dioxide (CO2) [2]. It is estimated that producing one ton of OPC releases about one ton of CO<sub>2</sub> [3]. During the last 5 years since 2015, CO<sub>2</sub> from cement production grew by 1.8% a year, according to the International Energy Agency. The growth of CO<sub>2</sub> exacerbates global warming, causing an increase in climate anomalies and natural disasters. In addition to CO<sub>2</sub>, some harmful gases such as sulfur dioxide (SO<sub>2</sub>) are discharged into the air, causing harm to the environment. Moreover, cement production consumes a lot of energy and raw materials, resulting in a shortage of natural resources [4,5]. Therefore, a new production mode is urgently needed to replace the traditional OPC.

In order to meet the requirements of the building materials industry for energy conservation and environmental protection, researchers have made continuous innovations and a lot of research results [6]. In 1979, French material scientist Davidovits first proposed the concept of geopolymer [7]. Geopolymer has a three-dimensional amorphous structure, which is a special aluminum silicate material. It is formed by alkali-activated solutions (AAS) and a

**Peng Zhang, Jia Su, Tianhang Zhang, Peng Zhang:** School of Water Conservancy and Transportation, Zhengzhou University, Zhengzhou, Henan 450001, China

possibility of applying MS-GPM in practical engineering by designing reasonable  $r_{\rm sp}$ .

<sup>\*</sup> Corresponding author: Zhen Gao, School of Water Conservancy and Transportation, Zhengzhou University, Zhengzhou, Henan 450001, China, e-mail: gz12faafr@126.com

substance rich in aluminum and silicon. The whole process does not require the involvement of cement, thus meeting the needs of environmental protection [8]. Generally, AAS are prepared with sodium silicate (Na2SiO3) solutions and common strong alkalis such as sodium hydroxide (NaOH). Geopolymers are produced from a wide range of raw materials, usually industrial by-products such as rice husk ash, red mud, metakaolin (MK), fly ash (FA), and ground granulated blast furnace slag (GGBFS) [9,10]. It reduces the consumption of natural materials and increases the reuse of industrial by-products. Lots of research results have proved that geopolymer composites have good mechanical properties, low drying shrinkage, and outstanding durability in chlorine ion penetration resistance, acid resistance, and high-temperature resistance [11-15]. In addition, water in geopolymer composites helps mix materials during production, but does not participate in polymerization reactions, thus saving a certain amount of water. It is the opposite of water being involved in hydration reactions in cementitious composites [16,17].

Researchers have found that the physical and chemical performances of geopolymers are related to the properties of the raw materials [18,19]. FA is solid waste from coal combustion in industrial production. Silica and alumina in its main components can react with an alkaline solution to form an aluminum-silicate hydration gel [20,21]. MK is an anhydrous aluminosilicate material with an amorphous phase structure, which is highly reactive with alkaline solutions [22,23]. Rao et al. [24] investigated the acid resistance of geopolymer composites under ambient and thermal curing conditions. The composition of the sample was 80% of FA and 20% of GGBFS. The data indicated that penetration depth and compressive strength loss of geopolymer composites under normal temperature curing were smaller in longer acid corrosion environments. Gorhan and Kurklu [18] investigated the properties of MK-FA-based geopolymer mortar (GPM). According to values of compressive and flexural strength, the ideal proportion of MK replacing FA was 60%. As MK increased, the compressive strength of GPM increased. Both FA and MK fill the pores, thus making the microstructure more compact. In addition to the type of industrial by-products, the type of activator solution, the concentration of NaOH, and other factors also affect the performance of GPM [21]. In general, the ratio of fine aggregate to the precursor has a marked impact on the porosity and strength of mortar. As the proportion of fine aggregate increases, the geopolymer in the mortar is relatively reduced, which leads to an increase in porosity and a decrease in strength. Taking GPM as an example, John et al. [21] pointed out that the ratio of fine aggregate to the

precursor greatly affected the mechanical properties and durability of GPM. However, there are few research results about the effect of fine aggregate-precursor ratio on GPM, which needs further exploration.

In addition to the optimized binder, natural river sand (RS) is the preferred fine aggregate for concrete and mortar. According to a report released by the United Nations Environment Programme in 2022, 50 billion tons of sand are extracted annually. The huge consumption brings challenges to the development of the global economy and ecology [25]. The loss of natural RS can lead to a host of problems such as reduced water tables, ecosystem imbalances, and poor soil quality [26–28]. Therefore, a new type of alternative sand is urgently needed to alleviate the loss of fine aggregate. Manufactured sand (MS) is a rock with a particle size of less than 4.75 mm screened after the waste rocks mined by hand are broken. MS is angular and rough, so it is different from natural sand materials [29]. A great number of research results have indicated that MS can be used in cement-based composites as a viable alternative to the natural sand crisis. Ding et al. [29] explored the influence of MS on 388-day concrete compressive strength. The content of stone powder was variable, which was 5, 9, and 13%, respectively. The results showed that MS could be used as a substitute for natural RS, and the long-term compressive strength had little difference with that of ordinary concrete. Ltifi and Zafar [30] investigated the effect of MS on the durability of cement-based composites instead of siliconbased sand. Compared with silicon-based sand as fine aggregate, MS had better resistance to chloride ion penetration and chloride salt erosion but lower impermeability and carbonization resistance. Shen et al. [31] believed that the stone powder content could have an impact on the performance of concrete more than the particle shape of MS, and the content of 7.5% was the best. The interfacial transition zone of MS concrete is narrower, and its structure is denser. The earlier results indicate that MS is an alternative for fine aggregate in cementitious materials. Significantly, there is relatively little research on the effect of MS on GPM.

In order to fill the gap in the research of GPM with MS and avoid excessive exploitation of RS, 100% MS was used as fine aggregate, and industrial waste FA and MK were used as the precursor to prepare GPM, which explored the impact of sand–precursor ratio ( $r_{\rm sp}$ ) on mechanical properties and durability of MK-FA-based GPM with MS (MS-GPM). The research results can further prove that MS is a feasible substitute for natural RS and the influence rule of  $r_{\rm sp}$  on MS-GPM is obtained. It is of great significance for environmental protection and promotes the possibility of MS-GPM in practical applications.

# 2 Experiment procedure

#### 2.1 Materials

The raw materials of MS-GPM include MK. FA. Na<sub>2</sub>SiO<sub>3</sub> solution, NaOH, MS, and water. The chemical compositions of MK and FA are listed in Table 1. The physical properties of MK are listed in Table 2. The Class I FA is produced in the Luoyang power plant, China, and its physical properties are summarized in Table 3. Na<sub>2</sub>SiO<sub>3</sub> (SiO<sub>2</sub>/Na<sub>2</sub>O = 3.2, specific gravity: 1.38 and solid content: 34.3%) and flake NaOH (purity: 99%) are used as the alkali activator. MS (fineness modulus: 2.9, stone powder content: 6%, moisture content: 4.5% and apparent density: 1,820 kg·m<sup>-3</sup>) is produced in Xinxiang, China. As fine aggregate in MS-GPM, MS is derived from limestone fragments. In the rolling process of limestone, particles smaller than 0.075 mm with the same composition as the parent rock are called stone powder. Some study results have shown that a moderate content of stone powder is helpful for improving the particle size distribution and interface characteristics of cement-based composites with MS as fine aggregate, thus improving the fresh performance and hardening characteristics. Generally, to ensure that the compressive strength of MS concrete is unaffected, the content of stone powder should not exceed 13%. At the same time, 9% stone powder can enhance the workability of fresh concrete to the greatest extent [29]. Considering geopolymer properties, the content of stone powder is 6% in the experiment.

#### 2.2 Preparation of specimens

In this experiment,  $r_{\rm sp}$  is the ratio of MS to MK and FA. Significantly, fine aggregate is MS with different gradations, dust content, and particle size than natural sand. In the test, the minimum  $r_{\rm sp}$  was determined to be 1. Based on the  $r_{\rm sp}$  of 1,

Table 1: Chemical compositions of FA and MK (wt%)

Chemical compositions	Na <sub>2</sub> O & K <sub>2</sub> O	SiO <sub>2</sub>	Al <sub>2</sub> O <sub>3</sub>	Fe <sub>2</sub> O <sub>3</sub>	CaO & MgO	SO <sub>3</sub>
FA	4.4	51.5	18.5	6.70	12.5	0.21
MK	≤0.7	53.0	43.0	1.30	≤0.8	

Table 3: Physical properties of FA

Density	Packing	Consistency (%)	Water	
(g·cm <sup>-3</sup> )	density (%)		absorption (%)	
2.1	0.780	48.0	106	

water and MS were added into MS-GPM at the same time, and no segregation phenomenon was considered the standard. The maximum  $r_{\rm sp}$  of 5 was determined by testing whether the three-day compressive strength of MS-GPM was within the range of 5-10 MPa. Therefore, the ratios of five kinds of MS to MK and FA were set as 1, 2, 3, 4, and 5, respectively. The mass ratio of FA to MK is 3:7. By adding NaOH into the Na<sub>2</sub>SiO<sub>3</sub> solution, the AAS with the ratio of SiO<sub>2</sub>/Na<sub>2</sub>O of 1.3 was synthesized. The mix proportions of MS-GPM are shown in Table 4.

In order to better prepare MS-GPM, the preparation process is as follows. First, MK, FA and MS were poured into the mixer and stirred for 2 min. Then, the prefabricated AAS was poured into the mixer and stirred for about 3 min. Eventually, water was added and stirred. The mixture was shaped in the mold, which was cured at usual temperature for 24 h and de-molding. The MS-GPM were cured for 28 days, and relative humidity was greater than 95%. The overall working flow chart is shown in Figure 1.

#### 2.3 Test methods of MS-GPM

#### 2.3.1 Mechanical tests

The compressive strength test and the splitting tensile strength test refer to [G[T70-2009 [32] and GB/T7897-2008 [33],

Table 4: Mix proportions of MS-GPM (kg·m<sup>-3</sup>)

Number	MS/MK and FA ( $r_{ m sp}$ )	Na <sub>2</sub> SiO <sub>3</sub>	NaOH	MS	МК	FA	Water
Q-1	1	445	71	613	429	184	100
Q-2	2	445	71	1,226	429	184	108
Q-3	3	445	71	1,839	429	184	162
Q-4	4	445	71	2,452	429	184	216
Q-5	5	445	71	3,065	429	184	270

Table 2: Physical properties of MK

Particle size (μm) Whiteness (%)		Intensity activation index (%)	Loss on ignition (%)	
1.2	70–80	12	0.5	

4 — Peng Zhang et al. DE GRUYTER

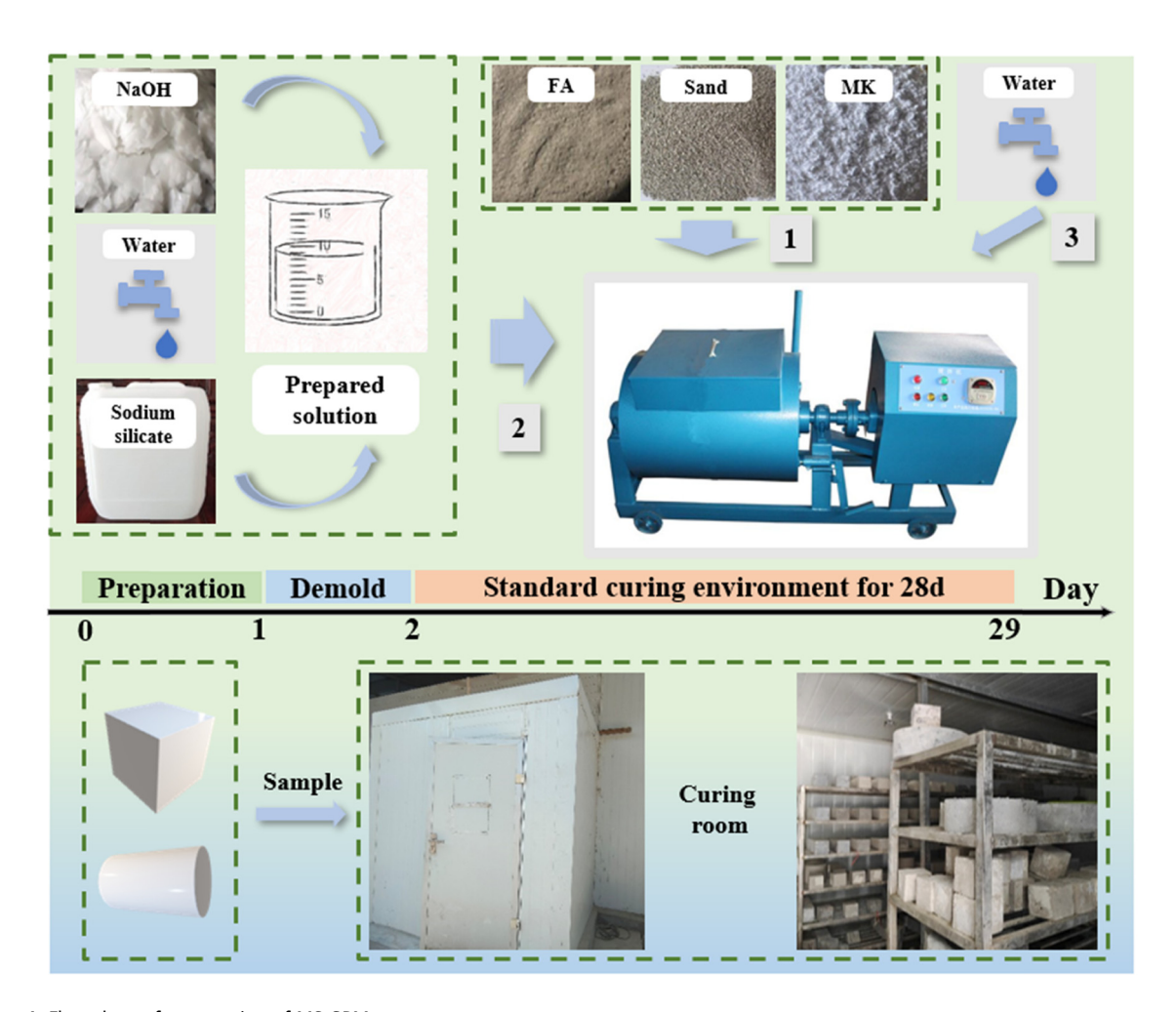


Figure 1: Flow chart of preparation of MS-GPM.

respectively. Three cube specimens were poured according to the mix ratio of each group in Table 4 with the size of 70.7 mm  $\times$  70.7 mm  $\times$  70.7 mm. The MS-GPM with the size of 40 mm  $\times$  40 mm  $\times$  160 mm was prepared according to the standard of GB/T7897-2008 [33] in the flexural and elastic modulus tests. The difference was that three cube specimens were poured in the mix ratio of each group for the flexural strength test, and six cube specimens were poured in the mix ratio of each group for the elastic modulus test, among which three were used to measure the axial compressive strength.

#### 2.3.2 Durability tests

The impermeability test of MS-GPM was conducted according to the standard GB/T50082-2009 [34]. Specimens with a size of  $185\,\mathrm{mm}\times175\,\mathrm{mm}\times150\,\mathrm{mm}$  were prepared to study the impermeability of MS-GPM, and 150 was the height of the platform. Six specimens were poured in each mix ratio. The penetration height method was used in the test, and the test device is

shown in Figure 2. After reaching the curing period, the MS-GPM specimens were put into the osmometer, gradually pressurized to 1.1 MPa and kept for 24 h. Finally, the specimens were split, and the penetration depth of each specimen was recorded, accurate to 0.1 mm. The equation for calculating the penetration depth of MS-GPM specimens is shown below:

$$\overline{D} = \frac{1}{6} \sum_{k=1}^{6} \overline{d_k},\tag{1}$$

where  $\overline{D}$  is the average penetration depth of a group of MS-GPM (mm), and  $\overline{d_k}$  is the penetration depth of the kth specimen in the group (mm).

Cracking resistance was tested according to specification JC/T951-2005 [35]. There were two specimens in each group, and the size was 910 mm  $\times$  600 mm  $\times$  20 mm. For cracking resistance tests, the test mold was placed in the center, and the MS-GPM was filled with the template and smoothed. After 24 h of continuous fan blowing, the transverse center of the wind speed should be controlled at 4–5 m·s<sup>-1</sup>. After the fan is turned off, turn on the iodine tungsten lamp above. Figure 3



Figure 2: Mortar penetrator and specimen size.

shows the crack resistance test layout. Finally, the length and width of the cracks were measured.

In this study, the cracking index  $W_c$  was used as the cracking resistance parameter of MS-GPM, and the calculation method was as follows:

$$W_{\rm c} = \sum {\rm Ai} \times {\rm Li},$$
 (2)

where  $W_c$  is the cracking index (mm), and Ai is the weight value corresponding to crack width on the surface of MS-GPM, which can be seen in Table 5, and Li is the crack length (mm).

#### 3 Results and discussion

# 3.1 Effect of $r_{sp}$ on mechanical properties of MS-GPM

#### 3.1.1 Compressive strength

The cube compressive strength changes of MS-GPM under five different MS to MK and FA ratios are illustrated in Figure 4. From Figure 4, the cube compressive strength of MS-GPM gradually decreases with the increase of  $r_{\rm sp}$ . When  $r_{\rm sp}$  was 1, the compressive strength of MS-GPM was the maximum, which was 40.2 MPa. When  $r_{\rm sp}$  was 2, 3, 4, and 5, the strength of MS-GPM was 34.7, 28.9, 16.5 and 8.6 MPa, which were reduced by 13.7, 28.1, 60.0, and 78.6% compared with the maximum value respectively. From the data, the increase of  $r_{\rm sp}$  in this study has negative impacts on the cube compressive strength of MS-GPM. Figure 5 shows the influence rule of  $r_{\rm sp}$  on failure morphology of MS-GPM specimen. As  $r_{\rm sp}$  increased, the damage of MS-GPM increased, and the crushing process extended from the edges to the interior with much less integrity. This is consistent with the pattern reflecting compressive

Table 5: Value corresponding to crack width weight

Crack width / (mm)	<i>l</i> < 0.5	<b>0.5</b> ≤ <i>l</i> < <b>1</b>	1 ≤ <i>l</i> < 2	2 ≤ <i>l</i> < 3	<i>l</i> ≥ 3
Ai	0.25	0.5	1	2	3

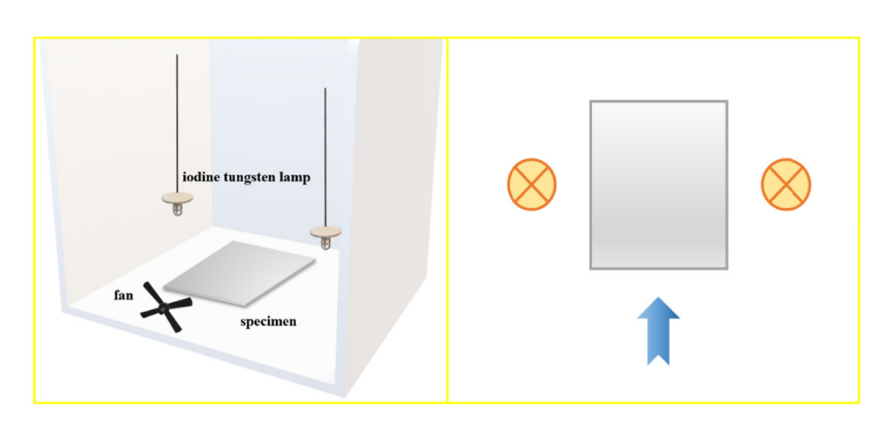


Figure 3: Cracking resistance test layout.

6 — Peng Zhang et al. DE GRUYTER

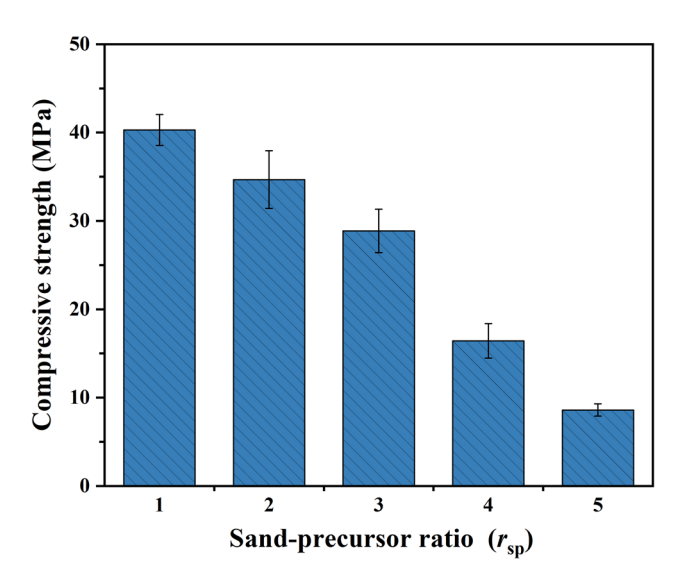


Figure 4: Compressive strength of MS-GPM.

strength. It is due to the fact that the strength of GPM depends on the amount of cementitious material on contact surfaces between MS and GPM. When the  $r_{\rm sp}$  is 1, there is more cementitious material on contact surfaces, so these surfaces are firmer and the compressive strength is maximum. The dosage of MS increases with the increase of  $r_{\rm sp}$ . The reduction of the proportion of cementitious material makes the weak interfacial transition zone (ITZ) more prone to micro-cracks, which reduces the strength of the matrix. In addition, due to some characteristics of MS itself that are weaker than RS, the reduction of compressive strength also has an impact.

Some researchers have also investigated the relationship between the compressive strength and  $r_{\rm sp}$  of GPM. Sashidhar *et al.* [36] explored the fresh performance and the compressive strength of self-compacting geopolymer

concrete (SCGC) by completely replacing natural RS with MS. The results showed that MS had no significant adverse impact on the preparation of SCGC. Colangelo et al. [37] performed experiments to test the compressive strength of GGBFS-FA based GPM at different curing temperatures by considering three different ratios of aggregates to GGBFS and FA (2, 1 and, 0.75). The result obtained is similar to MS-GPM. As the ratio decreased from 2 to 1, the compressive strength increased, but so did the compressive strength as the ratio continued to decrease. Temuujin et al. [38] prepared GPM with different amounts of sand, and the ratio of FA to sand was about 0.1-1. They revealed that the increase in the ratio had essentially no impact on the strength of GPM. Nematollahi et al. [39] reached the same conclusion. It was because the GPM of low aggregate content was similar to high aggregate content in bonding at the interface. They believed that the compressive strength of GPM was related not only to the aggregate itself, but also to the cementitious material and the interface combination of the two [40,41]. It is noteworthy that the amount of free water needs to be increased when the amount of MS is increased. It results in a decrease in compactness during solidification of MS-GPM, resulting in a decrease in compressive strength.

#### 3.1.2 Flexural and splitting tensile strength

Changes in flexural and splitting tensile strength of MS-GPM under different  $r_{\rm sp}$  are illustrated in Figures 6 and 7. As  $r_{\rm sp}$  increased, the flexural strength of MS-GPM decreased gradually from Figure 6. When  $r_{\rm sp}$  was 1, 2, 3, 4, and 5, the flexural strength was 4.3, 3.2, 2.8, 1.9, and 1.2 MPa. The minimum value was 72.1% lower than the maximum value. As is shown in Figure 7, the splitting tensile strength of



Figure 5: Failure modes of MS-GPM under different ratios of MS to MK and FA: (a) = 1; (b) = 3; (c) = 5.

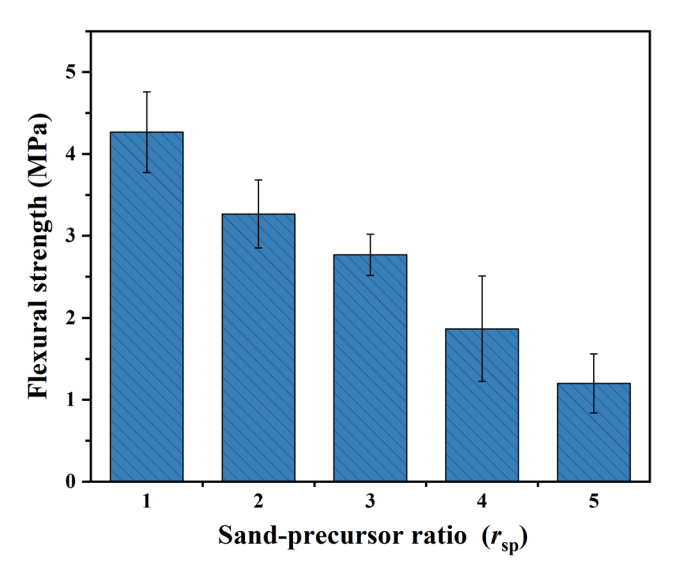


Figure 6: Flexural strength of MS-GPM.

MS-GPM decreases with increasing ratio. When  $r_{\rm sp}$  was 1, 2, 3, 4, and 5, the splitting tensile strength was 3.38, 3.13, 2.58, 1.45, and 0.98 MPa. The minimum value of 0.98 MPa was 71% lower than the maximum value of 3.38 MPa.

The above data show that the variation rule of flexural and tensile strength of MS-GPM is consistent with that of compressive strength [42-44]. Guades [45] set nine groups of RS to FA ratio (S/FA) and explored the influence of different S/FA on the splitting tensile strength of samples. Three ages were set up: 7, 14, and 28 days. When S/FA was 1.2, 2.0, 4.0, and 6.0, the 28-day tensile strength of the sample is 0.57, 0.46, 0.39, and 0.19 MPa, respectively. This is consistent with the variety rule of splitting tensile strength of MS-GPM, but its strength is much smaller than that of MS-GPM. First, according to the conclusion of Gorhan and Kurklu [18], the substitution of partial FA by MK improved the intensity of GPM, and the intensity growth rate of MK-FA-based GPM was higher [46,47]. Second, the ratio of Na<sub>2</sub>SiO<sub>3</sub> to NaOH solution is an essential element influencing the strength. In the GPM experiment of partial replacement of FA by GGBFS, Madhav et al. [48] found that the strength of GPM increased when the ratio of Na<sub>2</sub>SiO<sub>3</sub> to NaOH increased from 1 to 2. El-Hassan and Ismail [49] revealed that the strength increased faster when the ratio of Na<sub>2</sub>SiO<sub>3</sub> to NaOH was 2.5. The increase in strength is attributed to the increase in matrix reaction rate and the enhancement of precursor dissolution during polycondensation [21]. In addition to the previously mentioned reasons for poor flexural strength between aggregate and matrix due to insufficient cementing material, the increase in S/FA decreases the flow value and thus the tensile strength [45].

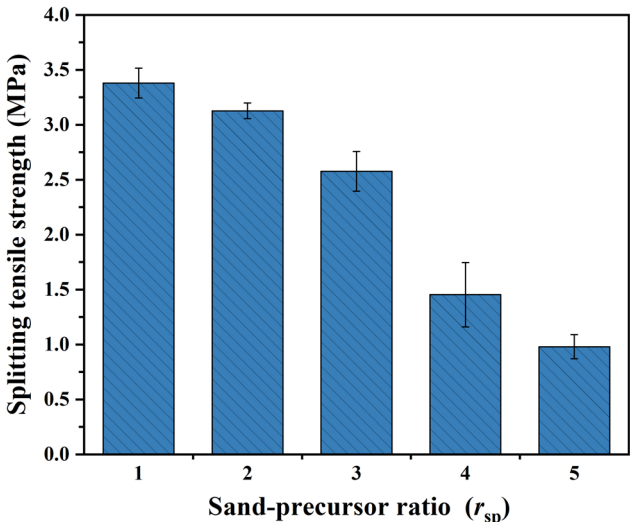


Figure 7: Splitting tensile strength of MS-GPM.

#### 3.1.3 Elastic modulus

Elastic modulus is one of the indexes to evaluate the deformation resistance of mortar and is closely related to the compressive strength [8,50,51]. The change of elastic modulus of MS-GPM with  $r_{\rm sp}$  is illustrated in Figure 8. From Figure 8, the elastic modulus decreased with increasing  $r_{\rm sp}$ . When  $r_{\rm sp}$  is 1, 2, 3, 4, and 5, the elastic modulus of MS-GPM is 4.7, 3.4, 1.9, 1.2, and 0.7 GPa. The minimum elastic modulus is reduced by 85.1% compared with the maximum. In a certain range, the increase of aggregate will reduce the elastic modulus of GPM. As mentioned earlier, MS has rough surfaces and irregular shapes. Temuujin  $et\ al.\ [38]$ 

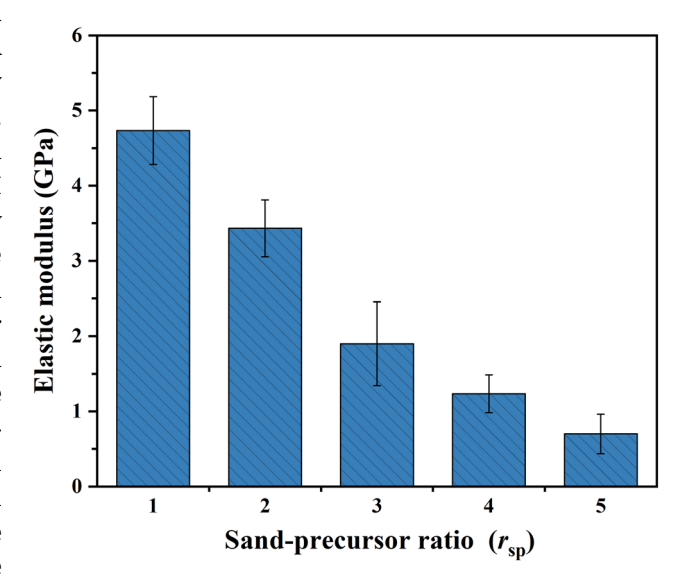


Figure 8: Elastic modulus of MS-GPM.

found that when the ratio of sand to FA was 0.1–1, the elastic modulus of GPM increased first and subtracted slightly when the ratio increased. Steinerova [52] tested the elastic modulus of MK-based GPM using a four-point bending test. The results showed that the elastic modulus decreased from 50% sand content, and its maximum value was similar to that of MS-GPM. The increase of MS proportion decreases the internal symmetry of mortar, which leads to an increase in mortar voidage, and finally leads to a decrease in elastic modulus.

# 3.2 Relationship of compressive strength with tensile and flexural strength of MS-GPM

Regression equation is a mathematical expression that can reflect the relationship between two variables. Fitting the obtained mechanical performance test data of MS-GPM is helpful for inferring conclusions and predicting the properties of GPM. It has been proved that compressive strength is closely related to the tensile and flexural strength of cement-based composites. To explore the relationship between the mechanical properties of MS-GPM, the linear model was selected among the exponential, polynomial, and linear models. It is considered that the model is most consistent with the mechanical property relationship of MS-GPM. According to the strength of MS-GPM, the linear fitting equation was adopted:

$$f_{\rm t} = 0.07898 f_{\rm c} + 0.26781,$$
 (3)

where  $f_c$  is the compressive strength of MS-GPM (MPa), and  $f_t$  is tensile strength (MPa).

The corresponding fitting curve is shown in Figure 9. According to Figure 9, data coordinates of MS-GPM are evenly distributed on both sides of the fitting curve, proving that splitting tensile strength is closely related to compressive strength. The coefficient of determination  $R^2$  was 0.97, indicating a good correlation between the two.

In addition to splitting tensile strength, several recent results have demonstrated that the compressive strength of GPM is connected with flexural strength, porosity, and unit weight [53–56]. In this study, linear fitting was used to fit the flexural and compressive strength of MS-GPM, and the expression was obtained with  $R^2 = 0.91$ :

$$f_{\rm f} = 0.09147 f_{\rm c} + 0.31595,$$
 (4)

where  $f_{\rm f}$  is the flexural strength of MS-GPM (MPa).

From Figure 10, the flexural strength of MS-GPM is closely related to the compressive strength. However, the

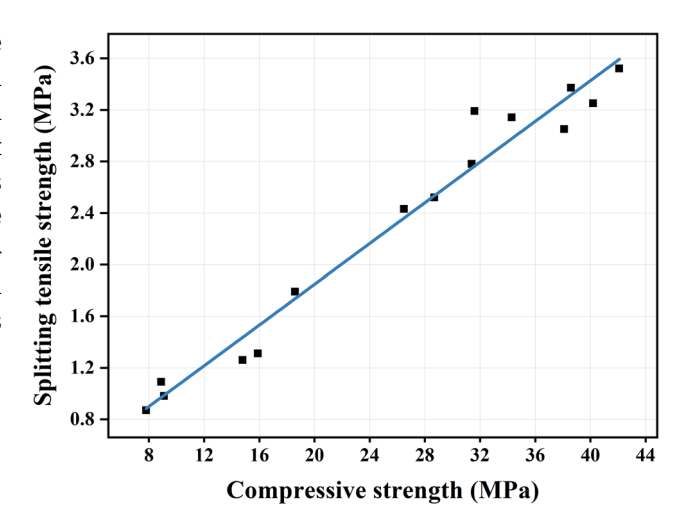


Figure 9: Linear fitting curve of MS-GPM.

data of MS-GPM are little and may lack uniformity. Therefore, the formula proposed in this article needs further validation.

As early as 2002, Zain *et al.* [57] speculated on the relationship between tensile and compressive strength of high-performance concrete (HPC) and obtained a relatively accurate Eq. (5):

$$f_{\text{ts},t} = 0.59 \sqrt{f'_{\text{c},t}} \left(\frac{t}{t_{28}}\right)^{0.04},$$
 (5)

where  $f'_{c,t}$  is the compressive strength (MPa),  $f_{ts,t}$  is the tensile strength of HPC on t days (MPa), t is the age of HPC specimen (d), and  $t_{28}$  is the age of HPC at 28 days (d).

Some scholars also use exponential fitting to explore the relationship between the two GPM. Ryu *et al.* [58] proposed the change equation of the tensile and compressive

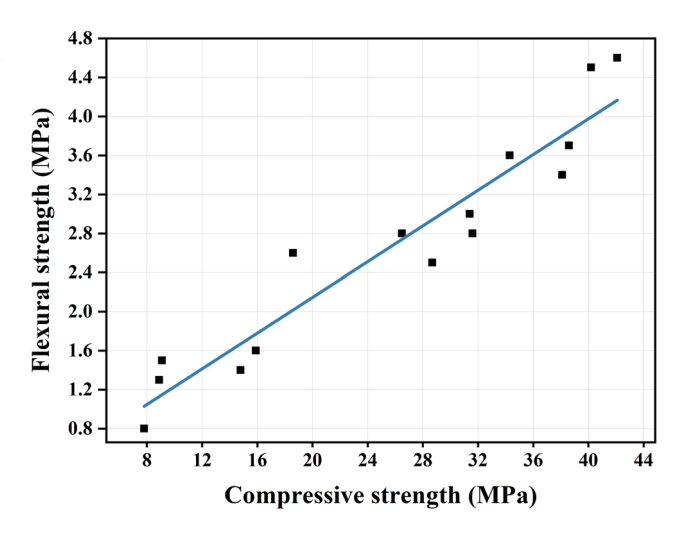


Figure 10: Linear fitting curve of MS-GPM.

strength of geopolymer concrete (GPC) and compared it with the fitting curve of Gardner and Poon [59] with a certain accuracy:

$$f_{\rm sp} = 0.17 (f_c')^{\frac{3}{4}},$$
 (6)

where  $f_{\rm sp}$  is the splitting tensile strength (MPa), and  $f_{\rm c}'$  is the compressive strength (MPa).

For linear fitting, Isa and Awang [60] predicted the relationship between the two of GPM using the palm oil fuel ash and GGBFS. Linear regression was adopted to better demonstrate the relationship between the two with  $R^2 = 0.95$ :

$$f_{\rm f} = 0.489 f_{\rm c} + 2.383,\tag{7}$$

where  $f_{\rm f}$  is the flexural strength of GPM (MPa).

For the equations of flexural and compressive strength, the 28-day compressive strength of GPM prepared by Isa and Awang [60] was generally lower than that of MS-GPM, but the maximum flexural strength was similar. Therefore, Eq. (7) has a higher slope. The preparation of AAS with wood ash (WA) instead of NaOH may be one of the reasons for the low compressive strength.

# 3.3 Effect of $r_{\rm sp}$ on durability of MS-GPM

#### 3.3.1 Water permeability

After dividing the MS-GPM specimen, the penetration depth was recorded, and the results are shown in Figure 11. It can be seen that the water penetration depth of MS-GPM

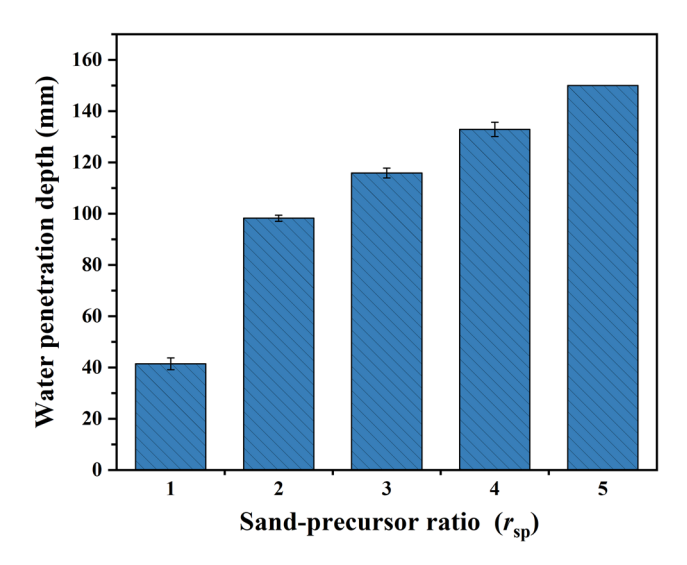


Figure 11: Water penetration depth of MS-GPM.

increases with the increase of  $r_{\rm sp}$ , which reflects the weakening of impermeability. When  $r_{\rm sp}$  was 5, the penetration depth of MS-GPM reached the maximum 150 mm, which was 108.7 mm higher than that when  $r_{\rm sp}$  was 1. Significantly, the impermeability of MS-GPM decreased greatly with  $r_{\rm sp}$  from 1 to 2, indicating that the distribution of MS, FA and MK in the matrix had a great influence on the impermeability of mortar. When the penetration depth is greater than 50 mm, the specimen should not be used as waterproof material [61]. Therefore, when  $r_{\rm sp}$  of MS-GPM is 1, the penetration depth is 41.3 mm, and it has good impermeability.

In fact, apart from some chemical corrosion, porosity is closely related to durability and especially impermeability [54,62]. On the one hand, MS-GPM with  $r_{\rm sp}$  of 1 has good impermeability, which can be attributed to the material itself. Saif et al. [55] suggested that the low permeability of the solution was due to the formation of dense alkali aluminosilicate gel (NASH) during the polymerization of MK-based GPM. Duan et al. [63] concluded that the pore structure could be optimized by partially replacing FA with MK. MK can play the advantage of fine particle size, fill the pores, and make the matrix more compact [64]. In addition, MgO and volcanic ash effect in FA also makes the matrix denser [65]. On the other hand, with the increase of  $r_{\rm sn}$ the deterioration of impermeability can be explained by the change in the specific gravity of MS and geopolymer. When  $r_{\rm sp}$  is 1, the cohesive force between MS particles is strong and the structure is dense. With the increase of MS proportion, the internal adhesion of the matrix becomes weak, the porosity increases, and the permeability becomes worse.

#### 3.3.2 Cracking resistance

According to the calculation method in 2.3.2, the cracking resistance of MS-GPM is represented by the cracking index. The relationship between the cracking index and  $r_{\rm sp}$  is shown in Figure 12. With the increase of  $r_{\rm sp}$ , the cracking index decreased gradually. When  $r_{\rm sp}$  was 1, 2, 3, 4, and 5, the cracking index of MS-GPM was 245, 226, 167, 126, and 36 mm, respectively. When  $r_{\rm sp}$  was 1, the cracking index reached the maximum value of 245 mm, which was 209 mm larger than the minimum value. The larger the cracking index is, the worse the cracking resistance is. Therefore, it can be concluded that the cracking resistance of MS-GPM increases with the increase of  $r_{\rm sp}$ .

With the increase of  $r_{\rm sp}$ , the effect of the MS skeleton is enhanced and the specific gravity of the matrix is decreased. Shariati *et al.* [66] pointed out that although the industrial by-products generated dense gel under the action of alkali

10 — Peng Zhang et al. DE GRUYTER

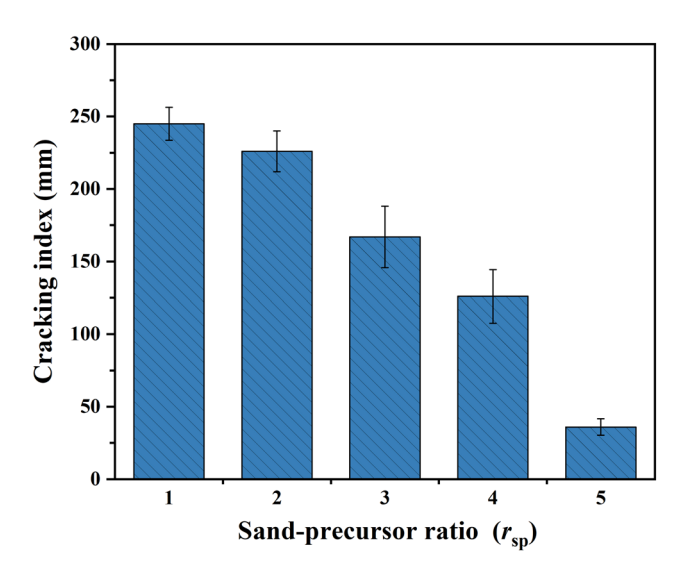


Figure 12: The cracking index of MS-GPM.

activation, there were still some particles and microcracks that were not fully reacted. It is also mentioned in the research of Saif et al. [55] and Zhang et al. [67]. These microcracks may be the cause of the cracking of MS-GPM. The reduction of the specific proportions of FA and MK also indirectly reduces the number of microcracks. In addition, the increase of the specific gravity of MS improves the bleeding of MS-GPM, which is beneficial to alleviate the plastic shrinkage stress caused by water loss, thus reducing the possibility of cracking. In fact, an increase in the waterbinder ratio will increase the water content during the plastic stage of MS-GPM, leading to a decrease in the filling rate of hydration products and promoting matrix cracking. But at the same time, the plastic shrinkage stress caused by water loss is reduced, and the cracking is alleviated. When the latter plays a dominant role, the increase of water permeability will enhance the crack resistance of MS-GPM.

## 3.4 Analysis of variance (ANOVA)

The ANOVA was invented by the British statistician and geneticist Ronald Fisher. It can be used to test the significance of differences between two or more sample means. In other words, the role of ANOVA lies in its ability to quantitatively present the effects of various factors on the subject, thereby improving the accuracy of data analysis. F-test is applicable to models with multiple parameters, also known as the ratio of variance. The statistic satisfies the Fdistribution under the null hypothesis. Kelestemur et al. [68] used ANOVA to discuss the influence of glass fiber content and other three factors on compressive and flexural strength, and found the most obvious influencing factors. Yan et al. [69] proved by ANOVA and F-test that silicate modulus had no obvious effect on the elastic properties of MK-based geopolymers. Therefore, ANOVA is very favorable for the response of statistical variables to the whole. To explore the influence of  $r_{\rm sn}$ on properties of MS-GPM, ANOVA and F-test were also used in the research. The value of F was calculated by Eq. (8).

$$F = \frac{\text{MS}_{\text{level}}}{\text{MS}_{\text{error}}} = \frac{\text{SS}_{\text{level}}/(N_{\text{level}} - 1)}{\text{SS}_{\text{error}}/(N_{\text{sample}} - N_{\text{level}})},$$
(8)

where  $MS_{level}$  and  $MS_{error}$  are the mean squares between and within groups,  $SS_{level}$  and  $SS_{error}$  are the sum of squares between and within groups,  $N_{level}$  is the number of layers in the sample, and  $N_{sample}$  is the number of samples.

The ANOVA results of MS-GPM with five  $r_{\rm sp}$  are shown in Table 6. The  $\alpha$  is taken to be 0.05. The p-value is a parameter used to determine the results of a hypothesis test. It is the level of significance calculated from the actual statistics. The confidence level for the F-test is 95%. If the calculated value F is greater than the critical value F according to the distribution of degrees of freedom, it can be proved that  $r_{\rm sp}$  has great effects on the performance of MS-GPM. Taking the compressive strength as an

Table 6: The results of ANOVA for MS-GPM

Performance indices	SS <sub>level</sub>	N <sub>level</sub>	SS <sub>error</sub>	N <sub>sample</sub>	MS <sub>level</sub>	MS <sub>error</sub>	F <sub>Calculated</sub>	<b>F</b> <sub>Critical</sub>	Significance
Compressive strength	2045.529	5	48.140	15	511.382	4.814	106.228	3.48	Significance
Splitting tensile strength	13.157	5	0.308	15	3.289	0.031	106.721	3.48	Significance
Flexural strength	17.163	5	2.047	15	4.291	0.205	20.964	3.48	Significance
Elastic modulus	33.040	5	1.580	15	8.260	0.158	52.278	3.48	Significance
Water penetration depth	41864.558	5	91.705	30	10466.140	3.668	2853.209	2.76	Significance
Cracking index	84486	5	1148	10	21121.5	114.8	183.985	5.19	Significance

example, there were 5 groups with 3 samples in each group. SS<sub>level</sub> was the sum of squares calculated by taking 15 samples as a whole, which was 2045.529. SS<sub>error</sub> calculated the sum of squares for each group and then added the sum of squares for the five groups to get 48.140.  $F_{\text{Calculated}}$  of 106.228 was greater than  $F_{\text{Critical}}$  of 3.48, which proved that  $r_{\rm sp}$  had great effects on the compressive strength of MS-GPM. In conclusion, the  $r_{\rm sp}$  significantly affects the compressive strength, flexural strength, splitting tensile strength, elastic modulus, impermeability, and cracking resistance of MS-GPM in the range of 1-5.

## 4 Conclusions

**DE GRUYTER** 

In the present study, the impact of  $r_{
m sp}$  on the influence rule and mechanism of MS-GPM was analyzed through the tests of compressive strength, splitting tensile strength, flexural strength, elastic modulus, impermeability, and cracking resistance. The results show that MS-GPM has excellent strength and durability. Based on the results, the conclusions could be listed:

- 1) The mechanical strength of MS-GPM decreased when  $r_{\rm sp}$ increased. When  $r_{\rm sp}$  was 1, MS-GPM had the highest strength and the best impermeability. The compressive strength, splitting tensile strength, flexural strength, and elastic modulus were 40.3 MPa, 3.4 MPa, 4.27 MPa and 4.7 GPa when  $r_{\rm sp}$  was 1. The cracking resistance of MS-GPM increased with the increase of  $r_{\rm sp}$ .
- 2) Compressive strength of MS-GPM is correlated with splitting tensile and flexural strength, which was proved by linear fitting. In addition, according to the results of ANOVA and F-test, the  $r_{\rm sp}$  in the range of 1–5 has great effects on the performance of MS-GPM.
- 3) Although the study concludes that when  $r_{\rm sp}$  is 1, the strength and durability of MS-GPM reach the best, the condition when  $r_{\rm sp}$  is less than 1 has not been explored. It should be paid more attention to in future research.

Acknowledgments: The authors thank all the editors and the anonymous referees for their constructive comments and suggestions.

Funding information: The authors acknowledge the financial support received from the National Natural Science Foundation of China (Grant No. 52278283), and the Natural Science Foundation of Henan (Grant No. 232300421003).

Author contributions: All authors have accepted responsibility for the entire content of this manuscript and approved its submission.

Conflict of interest: The authors state no conflict of

# References

- Zhang, P., C. Wang, C. Wu, Y. Guo, Y. Li, and J. Guo, A review on the properties of concrete reinforced with recycled steel fiber from waste tires. Reviews on Advanced Materials Science, Vol. 61, 2022. pp. 276-291.
- Zhang, P., X. Y. Sun, F. Wang, and J. Wang. Mechanical properties and durability of geopolymer recycled aggregate concrete: A Review. Polymers, Vol. 15, 2023, id. 615.
- Gao, T., L. Shen, M. Shen, L. Liu, and F. Chen. Analysis of material [3] flow and consumption in cement production process. Journal of Cleaner Production, Vol. 112, 2016, pp. 553-565.
- [4] Zheng, Y., J. Zhuo, P. Zhang, and M. Ma. Mechanical properties and meso-microscopic mechanism of basalt fiber-reinforced recycled aggregate concrete. Journal of Cleaner Production, Vol. 370, 2022, id. 133555.
- Youssf, O., M. Elchalakani, R. Hassanli, R. Roychand, Y. Zhuge, R. J. [5] Gravina, et al. Mechanical performance and durability of geopolymer lightweight rubber concrete. Journal of Building Engineering, Vol. 45, 2022, id. 103608.
- Zhang, P., S. Wei, G. Cui, Y. Zhu, and J. Wang. Properties of fresh and hardened self-compacting concrete incorporating rice husk ash: A review. Reviews on Advanced Materials Science. Vol. 61, 2022. pp. 563-575.
- Davidovits, J. Geopolymers: Inorganic polymeric new materials. Journal of Thermal Analysis and Calorimetry, Vol. 37, 1991,
- Elhag, A. B., A. Raza, Q. Z. Khan, M. Abid, B. Masood, M. Arshad, et al. A critical review on mechanical, durability, and microstructural properties of industrial by-product-based geopolymer composites. Reviews on Advanced Materials Science, Vol. 62, 2023, pp. 1-38.
- Aygörmez, Y., O. Canpolat, and M. M. Al-mashhadani. A survey on one year strength performance of reinforced geopolymer composites. Construction and Building Materials, Vol. 264, 2020, id. 120267.
- Zhang, P., X. Han, Y. Zheng, J. Wan, and D. Hui. Effect of PVA fiber on mechanical properties of fly ash-based geopolymer concrete. Reviews on Advanced Materials Science, Vol. 60, 2021, pp. 418-437.
- [11] Carreño-Gallardo, C., A. Tejeda-Ochoa, O. I. Perez-Ordonez, J. E. Ledezma-Sillas, D. Lardizabal-Gutierrez, C. Prieto-Gomez, et al. In the CO<sub>2</sub> emission remediation by means of alternative geopolymers as substitutes for cements. Journal of Environmental Chemical Engineering, Vol. 6, 2018, pp. 4878-4884.
- Han, Q., P. Zhang, J. Wu, Y. Jing, D. Zhang, and T. Zhang. [12] Comprehensive review of the properties of fly ash-based geopolymer with additive of nano-SiO2. Nanotechnology Reviews, Vol. 11, 2022, pp. 1478-1498.

- [13] Albitar, M., M. S. Mohamed Ali, P. Visintin, and M. Drechsler. Durability evaluation of geopolymer and conventional concretes. Construction and Building Materials, Vol. 136, 2017, pp. 374–385.
- [14] Asadi, I., M. H. Baghban, M. Hashemi, N. Izadyar, and B. Sajadi. Phase change materials incorporated into geopolymer concrete for enhancing energy efficiency and sustainability of buildings: A review. Case Studies in Construction Materials, Vol. 17, 2022, id. e1162.
- [15] Izzat, A., A. Mohd, M. M.A. B. Abdullah, H. Kamarudin, L. Moga, G. Che, et al. Microstructural analysis of geopolymer and ordinary portland cement mortar exposed to sulfuric acid. *Materiale Plastice*, Vol. 50, 2013, pp. 171–174.
- [16] Zhang, P., M. Wang, X. Han, and Y. Zheng. A review on properties of cement-based composites doped with graphene. *Journal of Building Engineering*, Vol. 70, 2023, id. 106367.
- [17] Zhang, P., J. Su, J. Guo, and S. Hu. Influence of carbon nanotube on properties of concrete: A review. *Construction and Building Materials*, Vol. 369, 2023, id. 130388.
- [18] Gorhan, G. and G. Kurklu. Investigation of the effect of metakaolin substitution on physicomechanical properties of fly ash-based geopolymer mortars. *Materials Today: Proceedings*, Vol. 81, 2022, pp. 35–42.
- [19] Zhang, P., S. Y. Wei, Y. X. Zheng, F. Wang, and S. W. Hu. Effect of single and synergistic reinforcement of PVA fiber and nano-SiO₂ on workability and compressive strength of geopolymer composites. *Polymers*, Vol. 14, 2022, id. 3765.
- [20] Swanepoel, J. C. and C. A. Strydom. Utilisation of fly ash in a geopolymeric material. *Applied Geochemistry*, Vol. 17, 2002, pp. 1143–1148.
- [21] John, S. K., Y. Nadir, and K. Girija. Effect of source materials, additives on the mechanical properties and durability of fly ash and fly ash-slag geopolymer mortar: A review. *Construction and Building Materials*, Vol. 280, 2021, id. 122443.
- [22] Zhang, P., C. Wang, F. Wang, and P. Yuan. Influence of sodium silicate to precursor ratio on mechanical properties and durability of the metakaolin/fly ash alkali-activated sustainable mortar using manufactured sand. *Reviews on Advanced Materials Science*, Vol. 62, 2023, id. 20220330.
- [23] Zhang, P., Y. W. Sun, J. D. Wei, and T. H. Zhang. Research progress on properties of cement-based composites incorporating graphene oxide. *Reviews on Advanced Materials Science*, Vol. 62, 2023, id. 20220329.
- [24] Rao, J. V., K. Srinivasa Rao, and K. Rambabu. Performance of heat and ambient cured geopolymer concrete exposed to acid attack. Proceedings of the Institution of Civil Engineers – Construction Materials, Vol. 172, 2017, pp. 192–200.
- [25] Guo, X., J. Yang, and G. Xiong. Influence of supplementary cementitious materials on rheological properties of 3D printed fly ash based geopolymer. *Cement & Concrete Composites*, Vol. 114, 2020, id. 103820.
- [26] Li, D., Y. Pan, C. Liu, P. Chen, Y. Wu, J. Liu, et al. Optimal design of glazed hollow bead thermal insulation mortar containing fly ash and slag based on response surface methodology. *Reviews on Advanced Materials Science*, Vol. 62, 2023, pp. 1–13.
- [27] Anbarasan, I. and N. Soundarapandian. Investigation of mechanical and micro structural properties of geopolymer concrete blended by dredged marine sand and manufactured sand under ambient curing conditions. *Structural Concrete*, Vol. 21, 2020, pp. 992–1003.
- [28] Farahani, H. and S. Bayazidi. Modeling the assessment of socioeconomical and environmental impacts of sand mining on local

- communities: A case study of Villages Tatao River Bank in Northwestern part of Iran. *Resources Policy*, Vol. 55, 2018, pp. 87–95.
- [29] Ding, X., C. Li, Y. Xu, F. Li, and S. Zhao. Experimental study on long-term compressive strength of concrete with manufactured sand. Construction and Building Materials, Vol. 108, 2016, pp. 67–73.
- [30] Ltifi, M. and I. Zafar. Effect of total substitution of crushed limestone sand on concrete durability. European Journal of Environmental and Civil Engineering, Vol. 26, 2022, pp. 121–143.
- [31] Shen, W., Y. Liu, Z. Wang, L. Cao, D. Wu, Y. Wang, and X. Ji. Influence of manufactured sand's characteristics on its concrete performance. *Construction and Building Materials*, Vol. 172, 2018, pp. 574–583.
- [32] JGJ/T 70-2009. Standard for test method of performance on building mortar. Architecture and Building Press, Beijing, China, 2009.
- [33] GB/T 7897–2008. Test methods of mechanical properties of mortar for ferrocement (In Chinese). China Standards Press, Beijing, China, 2008.
- [34] GB/T 50082-2009. Standard for test methods of long-term performance and durability of ordinary concrete (In Chinese). China Standards Press, Beijing, China, 2009.
- [35] JC/T 951-2005. *Test method for cracking-resistance of cement mortar*. China Architecture and Building Press, Beijing, China, 2005.
- [36] Sashidhar, C., J. Jawahar, C. Neelima, and D. Pavan Kumar. Fresh and strength properties of self compacting geopolymer concrete using manufactured sand. *International Journal of Chem Tech Research*, Vol. 8, 2015, pp. 974–4290.
- [37] Colangelo, F., R. Cioffi, G. Roviello, I. Capasso, D. Caputo, P. Aprea, B. Liguori, and C. Ferone. Thermal cycling stability of fly ash based geopolymer mortars. *Composites Part B: Engineering*, Vol. 129, 2017, pp. 11–17.
- [38] Temuujin, J., A. van Riessen, and K. J. D. MacKenzie. Preparation and characterisation of fly ash based geopolymer mortars. *Construction and Building Materials*, Vol. 24, 2010, pp. 1906–1910.
- [39] Nematollahi, B., J. Sanjayan, and F. U.A. Shaikh. Matrix design of strain hardening fiber reinforced engineered geopolymer composite. *Composites Part B: Engineering*, Vol. 89, 2016, pp. 253–265.
- [40] Lee, W. K. W. and J. S. J. van Deventer. The interface between natural siliceous aggregates and geopolymers. *Cement and Concrete Research*, Vol. 34, 2004, pp. 195–206.
- [41] Barbosa, V. F. F. and K. J. D. MacKenzie. Thermal behaviour of inorganic geopolymers and composites derived from sodium polysialate. *Materials Research Bulletin*, Vol. 38, 2003, pp. 319–331.
- [42] Meng, Z., L. Li, M. U. Farooqi, L. Feng, and L. Wang. Fiber factor for fresh and hardened properties of polyethylene fiber-reinforced geopolymer mortar. *Journal of Building Engineering*, Vol. 53, 2022, id. 104556.
- [43] Ren, R. and L. Li. Impact of polyethylene fiber reinforcing index on the flexural toughness of geopolymer mortar. *Journal of Building Engineering*, Vol. 57, 2022, id. 104943.
- [44] Zhang, P., C. Wang, Z. Gao, and F. Wang. A review on fracture properties of steel fiber reinforced concrete. *Journal of Building Engineering*, Vol. 67, 2023, id. 105975.
- [45] Guades, E. J. Experimental investigation of the compressive and tensile strengths of geopolymer mortar: The effect of sand/fly ash (S/FA) ratio. Construction and Building Materials, Vol. 127, 2016, pp. 484–493.
- [46] Jithendra, C., V. N. Dalawai, and S. Elavenil. Effects of metakaolin and sodium silicate solution on workability and compressive strength of sustainable geopolymer mortar. *Materials Today: Proceedings*, Vol. 51, 2022, pp. 1580–1584.

- [47] Kim, B. and S. Lee. Review on characteristics of metakaolin-based geopolymer and fast setting. Journal of the Korean Ceramic Society, Vol. 57, 2020, pp. 368-377.
- [48] Madhav, T. V., C. R. Krishna, I. V. R. Reddy, and V. G. Ghorpade. Study on compressive strength of geopolymer mortar. Advanced Materials Research, Vol. 935, 2014, pp. 163-167.
- [49] El-Hassan, H. and N. Ismail. Effect of process parameters on the performance of fly ash/GGBS blended geopolymer composites. Journal of Sustainable Cement-Based Materials, Vol. 7, 2018, pp. 122-140.
- [50] Nath, P. and P. K. Sarker. Flexural strength and elastic modulus of ambient-cured blended low-calcium fly ash geopolymer concrete. Construction and Building Materials, Vol. 130, 2017, pp. 22-31.
- [51] Wang, Y., S. Hu, and X. Sun. Experimental investigation on the elastic modulus and fracture properties of basalt fiber-reinforced fly ash geopolymer concrete. Construction and Building Materials, Vol. 338, 2022, id. 127570.
- [52] Steinerova, M. Mechanical properties of geopolymer mortars in relation to their porous structure. Ceramics Silikaty, Vol. 55, 2011,
- [53] Zhang, P., X. Han, J. Guo, and S. Hu. High-temperature behavior of geopolymer mortar containing nano-silica. Construction and Building Materials, Vol. 364, 2023, id. 129983.
- [54] John, S. K., Y. Nadir, A. Cascardi, M. M. Arif, and K. Girija. Effect of addition of nanoclay and SBR latex on fly ash-slag geopolymer mortar. Journal of Building Engineering, Vol. 66, 2023, id. 105875.
- [55] Saif, M. S., M. O. R. El-Hariri, A. I. Sarie-Eldin, B. A. Tayeh, and M. F. Farag. Impact of Ca + content and curing condition on durability performance of metakaolin-based geopolymer mortars. Case Studies in Construction Materials, Vol. 16, 2022, id. e922.
- [56] Karakaş, H., S. İlkentapar, U. Durak, E. Örklemez, S. Özuzun, O. Karahan, et al. Properties of fly ash-based lightweight-geopolymer mortars containing perlite aggregates: Mechanical, microstructure, and thermal conductivity coefficient. Construction and Building Materials, Vol. 362, 2023, id. 129717.
- [57] Zain, M. F. M., H. B. Mahmud, A. Ilham, and M. Faizal. Prediction of splitting tensile strength of high-performance concrete. Cement and Concrete Research, Vol. 32, 2002, pp. 1251-1258.
- [58] Ryu, G. S., Y. B. Lee, K. T. Koh, and Y. S. Chung. The mechanical properties of fly ash-based geopolymer concrete with alkaline activators. Construction and Building Materials, Vol. 47, 2013, pp. 409-418.

- [59] Gardner, N. J. and S. M. Poon. Time and temperature effects on tensile, bond, and compressive strengths. ACI Journal Proceedings, Vol. 73, 1976, pp. 405-409.
- [60] Isa, M. N. and H. Awang. Characteristics of palm oil fuel ash geopolymer mortar activated with wood ash lye cured at ambient temperature. Journal of Building Engineering, Vol. 66, 2023,
- Hedegaard, S. E. and T. C. Hansen. Water permeability of fly ash [61] concretes. Materials and Structures, Vol. 25, 1992, pp. 381-387.
- [62] Zhang, P., S. Wei, J. Wu, Y. Zhang, and Y. Zheng. Investigation of mechanical properties of PVA fiber-reinforced cementitious composites under the coupling effect of wet-thermal and chloride salt environment. Case Studies in Construction Materials, Vol. 17, 2022, id. e1325.
- [63] Duan, P., C. Yan, and W. Zhou. Influence of partial replacement of fly ash by metakaolin on mechanical properties and microstructure of fly ash geopolymer paste exposed to sulfate attack. Ceramics International, Vol. 42, 2016, pp. 3504-3517.
- [64] Jindal, B.B. Investigations on the properties of geopolymer mortar and concrete with mineral admixtures: A review. Construction and Building Materials, Vol. 227, 2019, id. 116644.
- [65] Wang, L., X. Lu, L. Liu, J. Xiao, G. Zhang, F. Guo, et al. Influence of MgO on the hydration and shrinkage behavior of low heat Portland cement-based materials via pore structural and fractal analysis. Fractal and Fractional, Vol. 6, 2022, id. 40.
- [66] Shariati, M., A. Shariati, N. T. Trung, P. Shoaei, F. Ameri, N. Bahrami, et al. Alkali-activated slag (AAS) paste: Correlation between durability and microstructural characteristics. Construction and Building Materials, Vol. 267, 2021, id. 120886.
- Zhang, P., L. Kang, Y. Zheng, T. Zhang, and B. Zhang. Influence of SiO<sub>2</sub>/Na<sub>2</sub>O molar ratio on mechanical properties and durability of metakaolin-fly ash blend alkali-activated sustainable mortar incorporating manufactured sand. Journal of Materials Research and Technology, Vol. 18, 2022, pp. 3553-3563.
- [68] Keleştemur, O., S. Yildiz, B. Gökçer, and E. Arici. Statistical analysis for freeze-thaw resistance of cement mortars containing marble dust and glass fiber. Materials & Design, Vol. 60, 2014,
- [69] Yan, D., S. Chen, Q. Zeng, S. Xu, and H. Li. Correlating the elastic properties of metakaolin-based geopolymer with its composition. Materials & Design, Vol. 95, 2016, pp. 306-318.